

Figure S1 Freeze-fracture TEM images of arrangements of gap junction molecules on germ cell surfaces. (A) Low-magnification image to show distribution of loosely-aggregated large particles on the P-face of a germ cell. Several small clusters of particles may represent sites of nascent gap junction formation. (B) Diagram of (A) with particles indicated as black dots. (C, D) Second germ cell showing larger aggregations of particles. (E) Very large arrangement of pits on the E-face of the sheath, stretching across the entire length of a germ cell (arrowheads mark the limits of the sheath E-face profile). (E') Low-magnification image of (E). (F) Pits in (E) that likely correspond to gap junction particles are indicated with black dots.

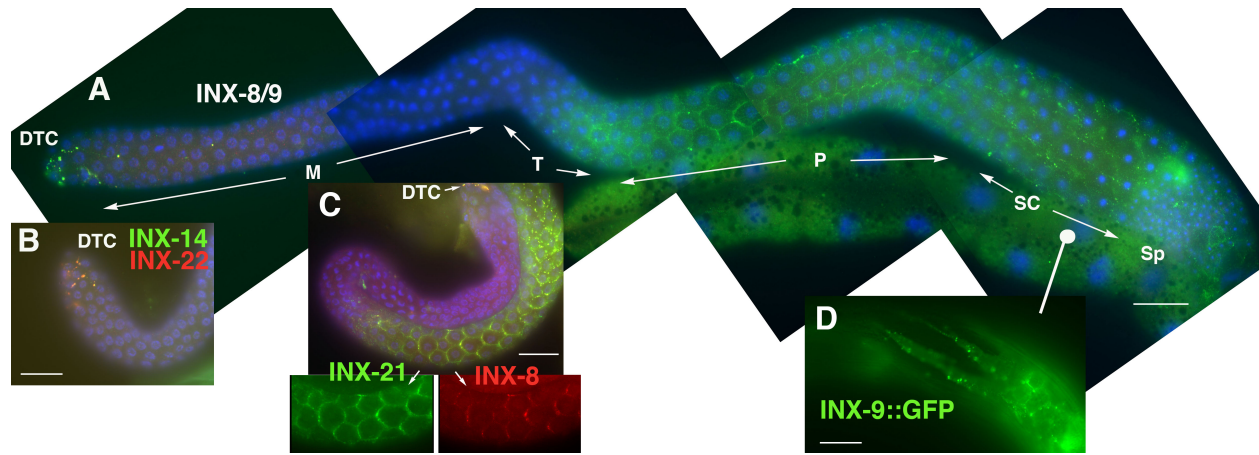


Figure S2 Distribution of innexins in the male gonad. (A) INX-8/9 is expressed in the DTCs, the pachytene region and the proximal arm. (B and C) Germ cell innexins colocalize with INX-8/9 in these same regions. (D) INX-9::GFP visualizes extensions of somatic cells in the region of the seminal vesicle. Scale bars, 20 μ m.

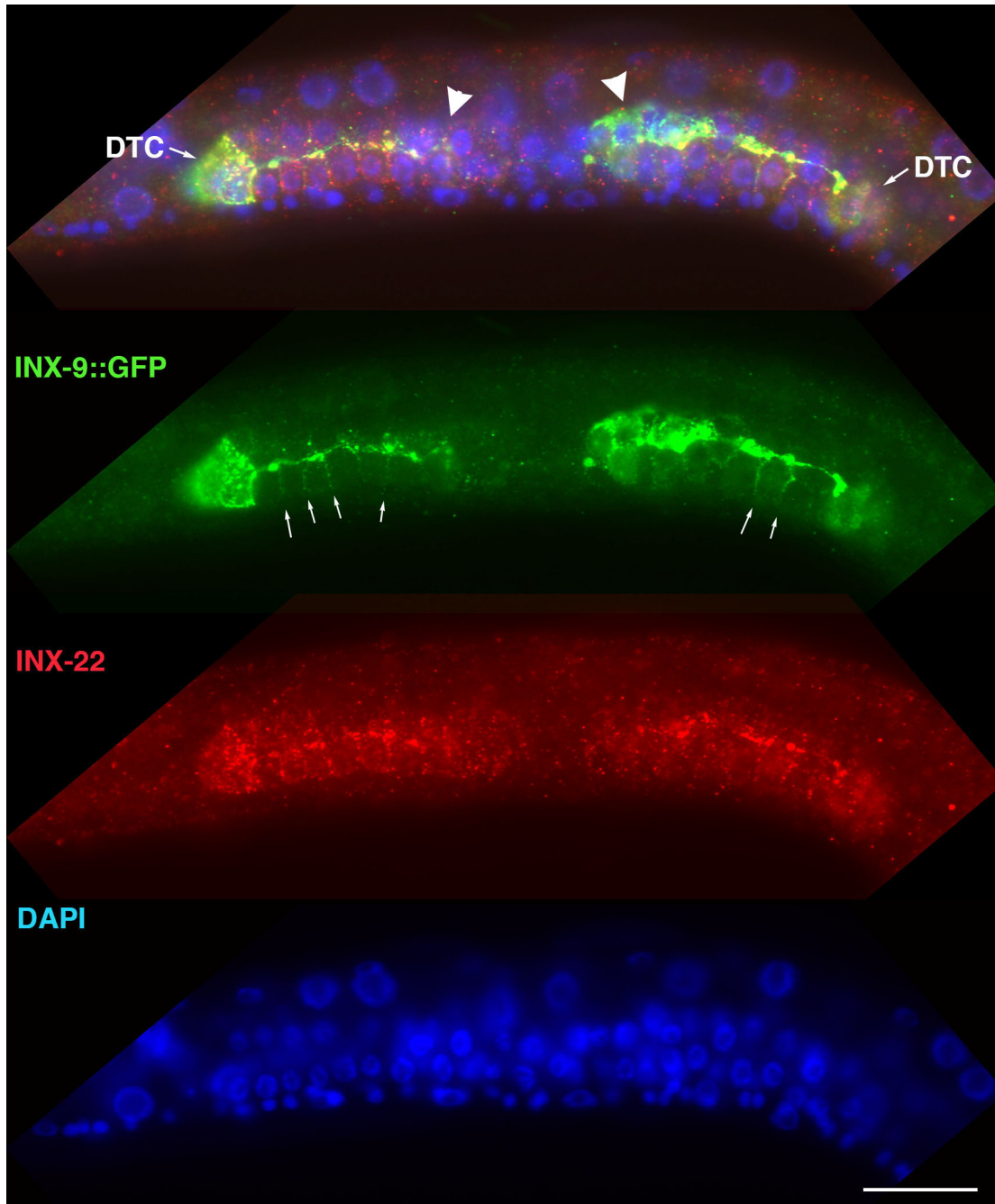


Figure S3 The DTC and other somatic cells establish gap junctions with most or all germ cells at the L2/L3 stage. A wild-type L2/L3 larva carrying *inx-9::gfp* was stained with anti-GFP and anti-INX-22 antibodies. A brightly-staining prominent process appears to emanate from each of the DTCs (the DTC associated with the right gonad arm lies out of this focal plane). As visualized in live animals, these large processes appear to run on the exterior surface of the germ cells, while other finer processes appear to radiate out from the large process and encircle the germ cells (small arrows). Other somatic gonad cells start to express *inx-9::gfp* at this time (arrowheads; cluster of cells in the left arm is just out of this focal plane), and it is unclear to what degree they may contribute to these processes. INX-22 and INX-9::GFP colocalize extensively along these processes; some tiny puncta can be detected along the finer processes, but their size suggests that gap junctions formed at this time may be small and masked by the strong diffuse expression signals detected for INX-9::GFP. Scale bar, 20 μ m.

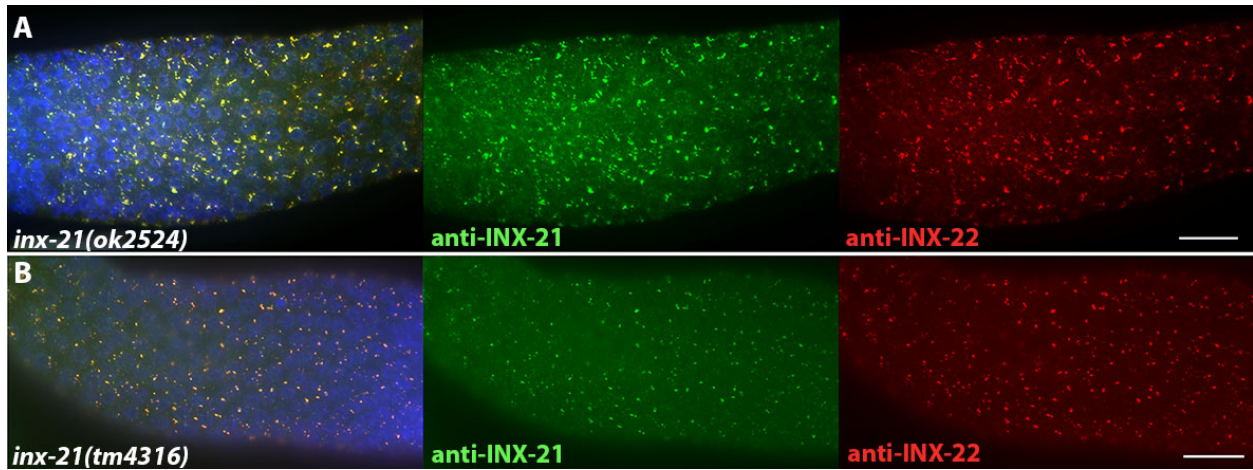


Figure S4 Anti-INX-21 antibodies detect punctate signals in *inx-21(ok2524)* (A) and *inx-21(tm4316)* (B) mutants that colocalize with INX-22. For technical reasons (i.e., *inx-21* null mutants are sterile and produce few germ cells), we cannot exclude the possibility that the anti-INX-21 sera cross reacts to some extent with INX-22 (the carboxyl termini of INX-21 and INX-22 share 26% identity). DAPI staining of nuclei is in blue. Scale bars, 20 μ m.

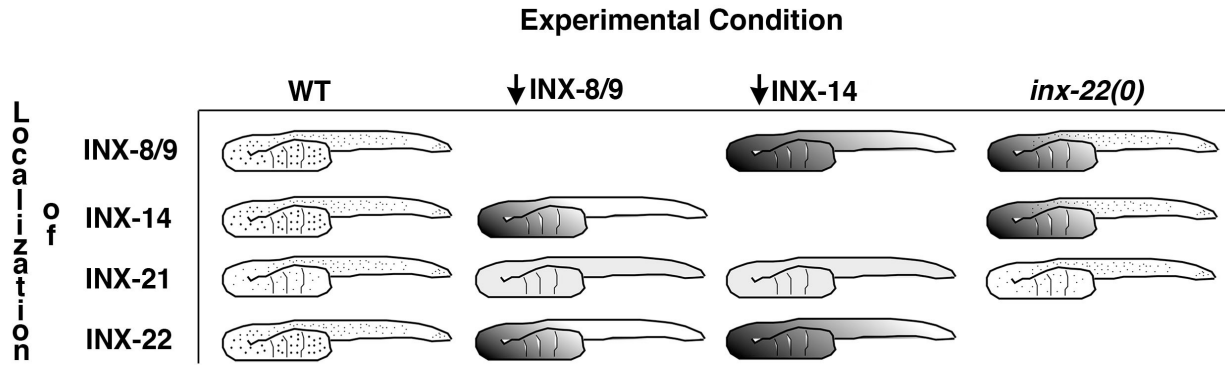


Figure S5 Summary of interdependence of innexin colocalization in the gonad. Because complete elimination of INX-8/9 or INX-14 produces gonad arms with few or no germ cells, we used experimental conditions to reduce expression of INX-8/9 and INX-14. These conditions included the examination of the hypomorphic *inx-14(ag17)* mutant, as well as animals that showed sufficient germ line proliferation to produce reflexed gonad arms after *inx-14(RNAi)* treatment of the wild type, or after *inx-8(RNAi)* treatment of *inx-9(ok1502)* mutants. In addition, we examined *inx-22(tm1661)* animals. An absence of innexin colocalization to puncta is interpreted as a reduction in gap junction formation. When puncta fail to form under these experimental conditions, expression of the non-targeted innexins can often be detected in a diffuse pattern (indicated as shading). Relatively high expression levels of INX-8/9, INX-14 and INX-22 in the proximal arm allow a strong signal to be detected even when diffuse, as indicated by darker shading; weaker diffuse expression in the distal arm, and for INX-21 throughout, is indicated as light shading.

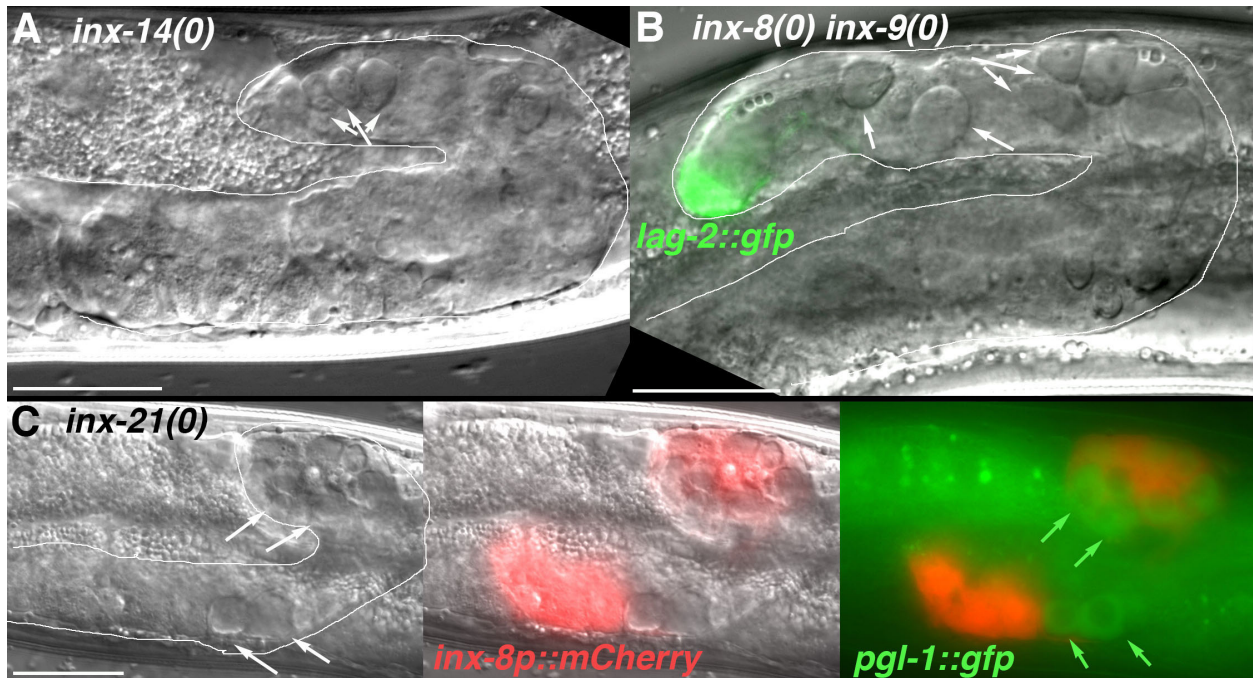


Figure S6 Germ cells in gonad innexin mutants become necrotic in adults. (A) *inx-14(tm2864)* gonad arm outlined, arrows point to a few of the necrotic foci. (B) *inx-8(tn1474) inx-9(ok1502)* with *lag-2::gfp* reporter marking the DTC and showing that germ cells, (arrows) but not the DTC, appear to undergo necrosis. (C) *inx-21(tn1540)* gonad arm expressing *inx-8p::mCherry* to visualize the DTC and sheath, and *pgl-1::gfp* to indicate germ cells. The distribution pattern of PGL-1::GFP is not particulate as in the wild type (see Figure 9C in the main text). Scale bars, 20 μ m.

Table S1 UDP-GlcNac injections rescue *gna-2(qa705)* mutants but not *inx-8(tn1474) inx-9(ok1502); tnEx205[lag-2p::inx-8::gfp)* mutants

Genotype	[UDP-GlcNac] injected ^a	Average number of progeny ^b
<i>gna-2(qa705) unc-55(e1170)</i>	uninjected	0 ± 0 (n=16)
	250 mM	3.0 ± 2.3 (n=23)
<i>inx-8(tn1474) inx-9(ok1502); tnEx205[lag-2p::inx-8::gfp)</i>	uninjected	0.6 ± 0.8 (n=15)
	100 mM	0.7 ± 0.9 (n=16)
	250 mM	0.4 ± 0.6 (n=20)

^aAdults were injected in a single gonad arm.

^bThe average number of hatched larvae.